

Triggering optical AGN: the need for cold gas, and the indirect roles of galaxy environment and interactions

J. Sabater^{1*}, P. N. Best¹ and T. M. Heckman²

¹*Institute for Astronomy (IfA), University of Edinburgh, Royal Observatory, Blackford Hill, EH9 3HJ Edinburgh, U.K.*

²*Center for Astrophysical Sciences, Department of Physics & Astronomy, The Johns Hopkins University, Baltimore, MD 21218, USA*

Accepted XXXX Month XX. Received XXXX Month XX; in original form XXXX Month XX

ABSTRACT

We present a study of the prevalence and luminosity of Active Galactic Nuclei (AGN; traced by optical spectra) as a function of both environment and galaxy interactions. For this study we used a sample of more than 250000 galaxies drawn from the Sloan Digital Sky Survey and, crucially, we controlled for the effect of both stellar mass and central star formation activity. Once these two factors are taken into account, the effect of the local density of galaxies and of one-on-one interactions is minimal in both the prevalence of AGN activity and AGN luminosity. This suggests that the level of nuclear activity depends primarily on the availability of cold gas in the nuclear regions of galaxies and that secular processes can drive the AGN activity in the majority of cases. Large scale environment and galaxy interactions only affect AGN activity in an indirect manner, by influencing the central gas supply.

Key words: galaxies: evolution – galaxies: interaction – galaxies: active – radio continuum: galaxies – surveys

1 INTRODUCTION

Active Galactic Nuclei (AGN) are closely linked to galaxy evolution and may play a fundamental role in the feedback processes that both quench the growth of massive galaxies (see reviews by Cattaneo et al. 2009; Heckman & Best 2014, and references therein) and establish the strong correlations between a galaxy’s black hole mass and the velocity dispersion of its stellar bulge (e.g. Marconi & Hunt 2003; Ferrarese & Merritt 2000; Gebhardt et al. 2000). The presence and characteristics of an AGN are tightly related to those of their parent galaxies, and nuclear activity has also been found to be linked to galaxy environment in several studies. Nuclear star formation (SF) activity is enhanced by interactions (see Li et al. 2008a, and references therein) as is expected from numerical simulations, but the dependence of AGN activity on environment is not so clear. Many apparently contradictory results are still found in the literature (see discussion in Sabater et al. 2013, hereafter SBA13).

An important point to consider is that the word “environment” is used to refer to at least two relevant but distinct aspects of galaxy environment: (a) the large scale environment, which effectively controls the gas supply to galaxies and, (b) one-on-one interactions, involving strong tidal interactions between companion galaxies. The relation of the prevalence of AGN with these two aspects can be differ-

ent or even opposite. For example, while the prevalence of radiatively efficient AGN decreases toward higher local densities of galaxies (Carter et al. 2001; Miller et al. 2003; Kauffmann et al. 2004), it is enhanced when one-on-one interactions are stronger (Petrosian 1982; Koulouridis et al. 2006; Alonso et al. 2007; Rogers et al. 2009; Ellison et al. 2011; Liu et al. 2012; Hwang et al. 2012). Hence, those different aspects of the environment should be considered separately (SBA13).

One of the most (if not the most) important factors that affects the triggering of an AGN is the galaxy mass. The prevalence of AGN depend strongly on the stellar (or black hole) mass of the host galaxy (e.g. Kauffmann et al. 2003; Best et al. 2005; Silverman et al. 2009; Tasse et al. 2011). The relation of the galaxy mass with the fraction of AGN is so strong that it will seriously bias any studies that do not take it into account properly. In SBA13, galaxy mass was accounted for using stratified statistical methods, and it was found that (at fixed mass) the prevalence of optical AGN is a factor 2–3 lower in the densest environments, but increases by a factor of ~ 2 in the presence of strong one-on-one interactions. The prevalence of AGN also depends on galaxy morphology (Moles et al. 1995; Schawinski et al. 2010; Sabater et al. 2012; Hwang et al. 2012) which is closely related to the star formation (Lintott et al. 2008). In fact, Kauffmann et al. (2007) and LaMassa et al. (2013) show how AGN activity is better linked to the central star formation of the galaxy than to the general star formation.

* E-mail: jsm@roe.ac.uk (JS); pnb@roe.ac.uk (PNB)

Li et al. (2008b) found that, if the central star formation and the AGN prevalence are considered together, there is no enhancement of the nuclear activity in galaxies with close companions. Similarly, Reichard et al. (2009) found that the lopsidedness of a galaxy is related to an enhanced activity level of the central black hole but, if the age of the central stellar population is matched in the comparison, this enhancement is no longer visible. These findings would be related to the suggestion of Park & Choi (2009) that galaxy mass and morphology are the main factors determining the rest of the properties of galaxies. All of this may indicate that the observed environmental dependence of both AGN and central star formation arises from the same underlying mechanisms and that the environment affects the AGN activity only by affecting the gas supply. If this is correct, the trends of AGN fraction with large scale environment should also disappear when the central star formation rate is controlled together with galaxy mass. The goal of this study is to extend the analysis of SBA13 to test this hypothesis, and also to look independently at interactions.

AGN come in two flavours depending on their feeding mechanism (see Heckman & Best 2014, and references therein): (a) quasar or radiative mode, believed to be fuelled by cold gas, observed as X-ray AGN, optical AGN and high excitation radio galaxies, and, (b) radiatively inefficient or jet-mode, probably fuelled by gas cooling from hot halos, and observed primarily as low excitation radio galaxies. The relation of these two types of AGN with the environment and interactions can be different or even opposite, as shown in SBA13. We will focus in this study on radiatively efficient AGN which are supposed to be fuelled by the cold gas that can also trigger the central star formation that we aim to control for.

We aim to study the effect of different aspects of the environment on radiatively efficient nuclear activity after taking into account the effect of both the mass and the star formation activity. We characterize the environment for a sample of ≈ 270000 galaxies using both a local galaxy density parameter and a tracer of one-on-one interactions. The sample and the data used are described in Section 2. In Section 3, the relations between the prevalence of optically selected AGN and the environmental parameters is quantified and analysed. The results are discussed in Section 4 and the final conclusions are presented in Section 5. Throughout the paper, the following cosmological parameters are assumed: $\Omega_m = 0.3$, $\Omega_\Lambda = 0.7$ and $H_0 = 70 \text{ km s}^{-1} \text{ Mpc}^{-1}$.

2 THE SAMPLE AND THE DATA

We use the sample presented in SBA13. This sample was based on the seventh data release of the Sloan Digital Sky Survey (SDSS DR7; Abazajian et al. 2009). It is composed of galaxies in the main spectroscopic sample with magnitudes between 14.5 and 17.77 in r-band (Strauss et al. 2002) and with redshift between 0.03 and 0.1. The final number of galaxies in the sample is 267973.¹

We will use two of the environmental parameters derived in SBA13. In that study three environmental parameters were considered, to trace different aspects of the environment and interaction: (a) a local galaxy density parameter (hereafter “density”), (b) a tidal forces estimator, and (c) a cluster richness estimator (from Tago et al. 2010). The density parameter is derived from the density of galaxies up to the 10^{th} nearest neighbour; defined as $\log(10/\text{Vol}(r_{10^{\text{th}}}))$, where $r_{10^{\text{th}}}$ is the projected distance in Mpc to the 10^{th} companion. The tidal estimator traces the relation between the tidal forces exerted by companions and the internal binding forces of the galaxy; defined as $\log(\sum_i [(L_r/L_{r_i}) \times (2R/d_i)^3])$, where L_r is the luminosity in r-band of the galaxy, L_{r_i} the luminosity in r-band of the companion, R the radius of the galaxy and d_i the distance between the galaxy and the companion. A Principal Component Analysis (PCA) was applied to consider and remove the possible correlations between the environmental parameters. We found that the local density of companions around the target galaxy (a measure of the larger-scale environment in which the galaxy lives) is one of the main environmental driving factors for AGN activity and was well traced by the density parameter (also largely equivalent to the PCA1 component). We found that one-on-one interactions are also important driving factors, and are best traced by the the PCA component denominated PCA2 (defined as $0.707 \times \text{tidal} - 0.707 \times \text{density}$). PCA2 seems to take into account and corrects, at least partially, the possible 2D projection effects that would affect a pure tidal estimator in dense environments. Hence, we selected density and PCA2 for this study.

We also used the total stellar mass of the galaxy and the specific star formation rate measured in the central area covered by the spectrograph fibre (Kauffmann et al. 2003; Brinchmann et al. 2004; hereafter we will use sSFR to refer to this central measurement of the specific star formation rate: $\text{sSFR} = \text{nuclear star formation divided by total stellar mass}$). We will also use the optical AGN classification. A galaxy is considered to harbour an optical AGN if it is classified as a Seyfert, LINER or transition object using the standard emission line ratio diagnostic diagrams (e.g. Kewley et al. 2006) and the luminosity of its [O III] emission line is higher than $10^{6.5} L_\odot$. This limit selects only bright AGN but avoids the possible classification biases arising from the different redshifts of the galaxies of the sample (see SBA13). The number of AGN galaxies classified as each type using the former criteria are the following: 3347 Seyfert, 644 LINER, 1704 transition objects. The mean $L_{[\text{O III}]}$ of the AGN is 6.90 ± 0.34 . Note that because of the high $L_{[\text{O III}]}$ limit, the vast majority of the selected AGN are Seyferts, so this will be a study of radiatively efficient AGN, even if LINERs are classified as jet-mode AGN (Heckman & Best 2014).

There is a chance for relatively faint AGN to be misclassified as SF nuclei if their emission is concealed by the strong emission of a powerful star forming host. The high $L_{[\text{O III}]}$ limit helps to minimise the misclassification of AGN within galaxies with high star formation rates. Furthermore, for galaxies of a given mass and SFR, there is no reason to expect that any misclassification should be a function of environment. To check this, we examined AGN-tracers (e.g. $L_{[\text{O III}]}$) in the SF-classified galaxies in both high and

¹ There were duplicated data for 4 galaxies in the catalogue presented on SBA13. The indices of these galaxies are: 51930-285-80; 51999-286-559; 52173-644-540 and 52468-717-223 (mjd-plate-fiberid). The duplicate entries were removed from the catalogue.

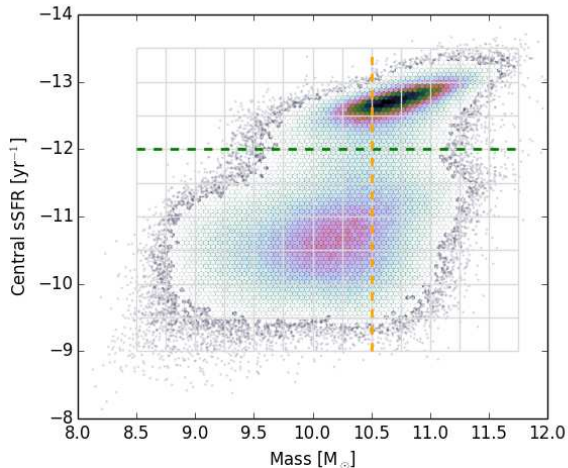


Figure 1. Distribution of mass and sSFR of the whole sample. The separation lines of $\text{sSFR} = 10^{-12} \text{ yr}^{-1}$ and $M = 10^{10.5} M_{\odot}$ are shown as dashed lines. The grid marks the bins used for some of the stratified statistical studies of Section 3 (see text).

low density (or PCA2) environments and found no evidence of any differences. We also confirmed that our results were unchanged (within the errors) if transition objects (a limit case mix of SF and AGN) were excluded from the analysis. Therefore, this effect should not affect the results.

The distribution of the mass and sSFR is shown in Fig. 1. The mass of the galaxies of the sample ranges from a minimum of $10^{8.1} M_{\odot}$ to a maximum of $10^{12.2} M_{\odot}$ with a mean of $10^{10.3} M_{\odot}$. The sSFR follows the well-established distribution (e.g. Strateva et al. 2001) with a star forming population ($\text{sSFR} \gtrsim 10^{-12} \text{ yr}^{-1}$) and a passive population ($\text{sSFR} \lesssim 10^{-12} \text{ yr}^{-1}$) and 99 per cent of the galaxies with values between $10^{-9.4} \text{ yr}^{-1}$ and $10^{-13.2} \text{ yr}^{-1}$. We will use a value of $\text{sSFR} = 10^{-12} \text{ yr}^{-1}$ to separate the high and low sSFR populations when needed. An additional separation in mass of $M = 10^{10.5} M_{\odot}$ will be used as well when required.

The relation of the environmental parameters, density and PCA2, with respect to the mass and the sSFR is shown in Fig. 2. The correlations are subtle but may be strong enough to bias the study if not taken into account at a later stage. The two sSFR populations are clearly visible on the upper panels. The high density end is populated by massive galaxies (visible on the lower-left panel) and these galaxies are mainly low sSFR galaxies (upper-left panel). There is a weak trend for low sSFR galaxies to be located at lower levels of PCA2 than high sSFR galaxies (upper-right panel).

Finally, for some computations we used the mass of the black hole, which was derived using the relation of McConnell & Ma (2013) as explained in Heckman & Best (2014). We also considered the bolometric luminosity of the AGN to be $L_{\text{bol}} = 3.5 \times 10^3 L_{[\text{O III}]}$, where $L_{[\text{O III}]}$ is not corrected for dust extinction.

3 RESULTS

We investigate the relation of the prevalence of optical AGN with the environmental parameters, density and PCA2, tak-

ing into account the effect of the mass and the sSFR. To do that, we compute the odds ratio of a galaxy harbouring an AGN at values of the environmental parameter above or below its median value (-0.603 for the density and -0.043 for PCA2; see Fig. 2). The masses are divided in strata of $0.25 M_{\odot}$ from $\log(M) = 8.50 [M_{\odot}]$ to $\log(M) = 11.75 [M_{\odot}]$, and the sSFR are divided in strata of $0.5 [\text{yr}^{-1}]$ from $\log(\text{sSFR}) = -13.5 [\text{yr}^{-1}]$ to $\log(\text{sSFR}) = -9.0 [\text{yr}^{-1}]$. The grid composed by the different strata is shown in Fig. 1. In each of these bins, a Fisher’s exact test is performed. We obtain the odds ratio (the strength of the relation between harbouring an AGN and a higher value of the environmental parameter; if this is ≈ 1 the chance of harbouring an optical AGN is the same at lower and higher values of the environmental parameter) and a p -value that indicates whether the trend found is significant.

The results of the Fisher’s test are shown in Fig. 3. For the density parameter, the odds ratios are usually close to 1 and the p -values are, in general, higher than 0.05 indicating that the possible trends are not significant. There is only one bin in the high sSFR and high mass region where the trend may be significant ($p \leq 0.01$) but the value of the odds ratio is not far from 1 in this case. We therefore find no significant trend of the prevalence of AGN with respect to the density. In the case of PCA2, we find a significant positive trend for one bin in the low sSFR and high mass region and a clearly significant negative trend for 4 bins in the high sSFR and low mass region.

It should be noted that the size of the bins may affect the statistics of the test. The bins need to be small to avoid biases due to strong trends of the fraction of AGN with mass, but the smaller the bins the lower the statistical significance of the test. Therefore, we will use a statistical method that aggregates the information of the bins to gain in statistical significance but that still accounts for the different strata used: the Cochran-Mantel-Haenszel test (CMH; Cochran 1954; Mantel & Haenszel 1959). It gives the strength of association between two bi-valued variables (odds ratio) and its statistical significance after taking into account the effects of the possible confounding factors defined as the strata.

It is also clear that the whole sample may not homogeneously follow a trend; that appears to be the case for PCA2 (right panel of Fig. 3). A Woolf’s test of homogeneity of odds ratios among strata (Woolf 1955) was applied to check whether the trends were homogeneous enough within the sample. A low p -value for this test means that the trends are different for different parts of the parameter space. Hence, we need to separate the analysis in different regions to obtain meaningful values of the CMH test. For density, we found no evidence of any heterogeneity. In the case of PCA2, we found signs of statistically significant heterogeneity using this test for the whole sample and also when considering only the high sSFR sub-sample. However, when splitting into four sub-samples, by mass and sSFR, no evidence of heterogeneity was found in PCA2 for any sub-sample.

We applied the CMH test to check for the significance of the relation between the presence of an optical AGN and values of the environmental parameters above or below their median. The confounding factors considered are again sSFR and mass. The test was applied to the complete sample, to the high and low sSFR sub-samples and to the four sub-

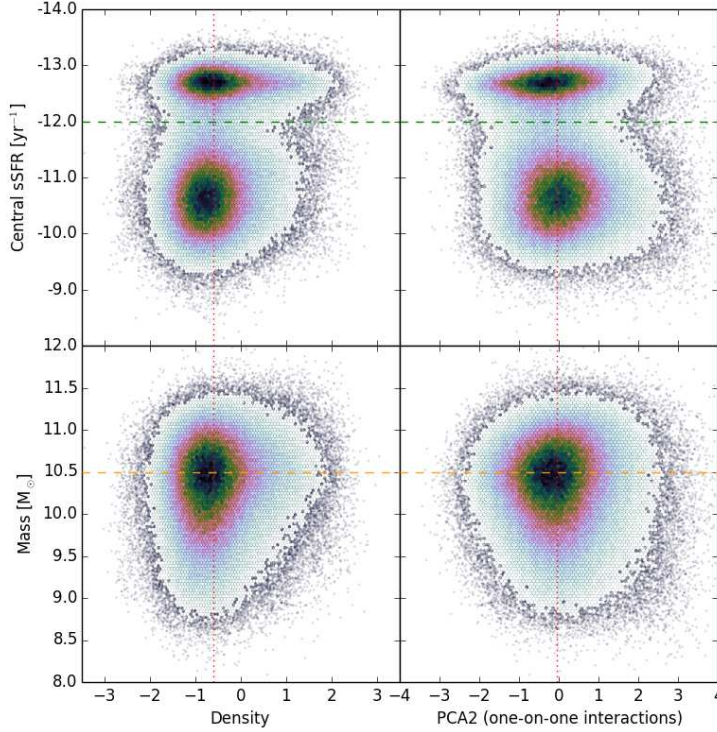


Figure 2. Distribution of mass, sSFR, density and PCA2 for the whole sample. The medians of the density and PCA2 are marked with dotted lines. The separation lines of $\text{sSFR} = 10^{-12} \text{ yr}^{-1}$ and $M = 10^{10.5} M_{\odot}$ are shown as dashed lines.

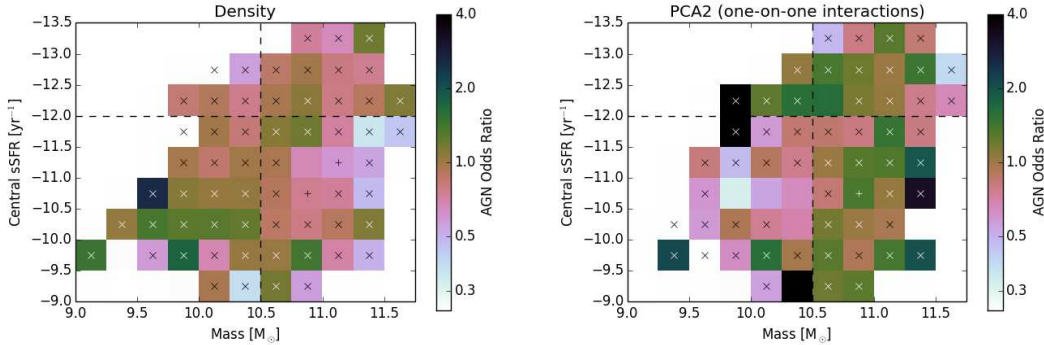


Figure 3. Odds ratios of the prevalence of AGN with respect to the level of density and one-on-one interactions (PCA2). The bins correspond to those shown in Fig. 1. An odds ratio lower than one indicates a negative relation between the probability of harbouring an AGN and a higher value of the environmental parameter; a value higher than one indicates a positive relation. Note that the statistical significance must be taken into account in order to interpret these relations. The bins for which the p -value is higher than 0.05 are marked with a cross and those in which the p -value is between 0.05 and 0.01 are marked with a plus sign. Only in the one (left panel) and six (right panel) bins with no symbol is the odds ratio significantly ($p \leq 0.01$) at variance with unity.

samples obtained with the $\text{sSFR} = 10^{-12} \text{ yr}^{-1}$ and $M = 10^{10.5} M_{\odot}$ separation lines. We checked that the results were not affected by the sizes of the bins. The results are the same using from 4 to 128 bins per sample or sub-sample.

The results of the CMH and the Woolf’s tests are shown in Table 1 and Fig. 4. The values of the ratios for the density are in general compatible with the absence of a clear trend. Even in the two cases where the deviation of the ratios from unity can be considered statistically significant, their values are very close to 1 implying changes in the probability of triggering an AGN of less than 10 per cent. In the case of

PCA2 the result for the whole sample is compatible with 1 but with heterogeneity. When the sample is separated by sSFR an opposite significant trend appears in the two sSFR regimes; galaxies with low sSFR and higher values of PCA2 harbour more AGN (about 20 per cent more when the value of PCA2 is above the mean). On the other hand, galaxies with high sSFR, especially galaxies with low mass and high sSFR seem to harbour fewer AGN in this case. The AGN prevalence is about 30 per cent higher at low than at high PCA2 values for high sSFR, low mass galaxies.

We checked the activity level of the AGN with respect

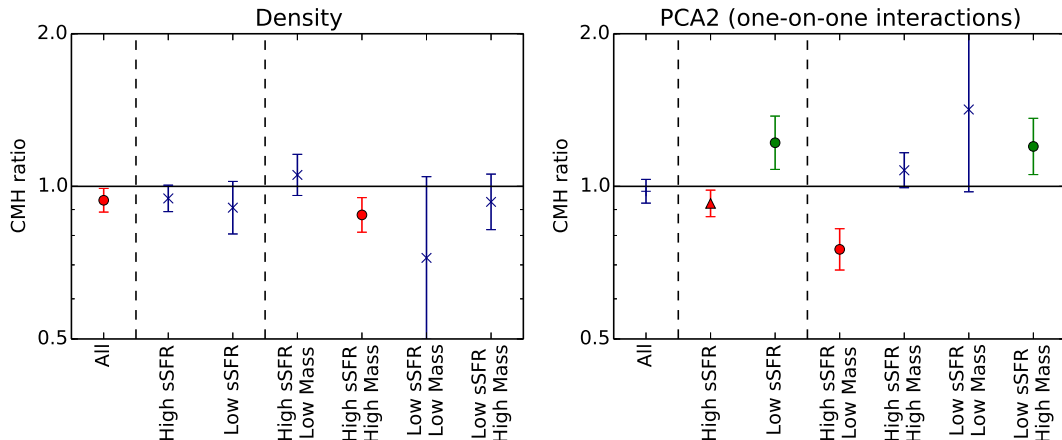


Figure 4. CMH ratios for the prevalence of optical AGN with respect to the density and one-on-one interactions (PCA2). The error bars mark the 95 per cent confidence interval. The shape of the symbol indicates if the trend found is statistically significant and if the data of the sample tested is homogeneous enough for the CMH ratio to be relevant (see text). Statistically significant trends ($p \leq 0.05$) are marked with solid symbols (triangles or circles). A value of the Woolf test below 0.05, indicating that the odds ratios are heterogeneous among the strata, is marked as a plus sign (instead of a cross) or a triangle (instead of a circle).

Table 1. Statistical study results from the CMH test. For each cell of the table the first row shows the CMH common odds ratio and its 95 per cent confidence interval and the second row shows the statistical significance or p -value (i.e., the probability of the trend occurring by chance) measured by the CMH test. The hypothesis tested was that the observed nuclear activity type is independent of the density or PCA2 parameter. The typeface of the p -value depends on its value: bold if $p < 0.01$; bold italics if $0.01 \leq p < 0.05$; and italics if $p \geq 0.05$. An asterisk marks the two results where the data is deemed as heterogeneous using the Woolf test.

	Density	PCA2
All	0.939 ± 0.049 <i>0.0214</i>	0.978 ± 0.051 * <i>0.4259</i>
High sSFR	0.947 ± 0.055 <i>0.0761</i>	0.925 ± 0.054 * <i>0.0124</i>
Low sSFR	0.91 ± 0.10 <i>0.1176</i>	1.22 ± 0.14 <i>0.0014</i>
High sSFR & Low Mass	1.053 ± 0.094 <i>0.2855</i>	0.751 ± 0.067 <i>0.0000</i>
High sSFR & High Mass	0.878 ± 0.066 <i>0.0013</i>	1.076 ± 0.082 <i>0.0741</i>
Low sSFR & Low Mass	0.72 ± 0.22 <i>0.1006</i>	1.42 ± 0.44 <i>0.0823</i>
Low sSFR & High Mass	0.93 ± 0.11 <i>0.2870</i>	1.20 ± 0.14 <i>0.0058</i>

to the environmental parameters. We computed the median of the logarithm of the [O III] luminosity per unit black hole mass, which is a measure of the Eddington-scaled accretion rate ($L_{\text{bol}}/L_{\text{Edd}} \sim 0.11L_{[\text{O III}]} / M_{\text{BH}}$), at different levels of the environmental parameters in the four different sub-samples. The results are shown in Fig. 5. The value of the median $\log(L_{[\text{O III}]} / M_{\text{BH}})$ does not show a significant trend with the density or PCA2 in any of the sub-samples and is, in general, compatible with the median value for each sub-sample. On the other hand, the median value can be seen to depend strongly on both the mass and sSFR, which are used to

define the sub-samples, emphasising the need to account for these parameters.

Finally, we checked if any possible contamination by jet mode AGN was affecting our results. We applied a cut-off on the accretion rate of the AGN selecting only galaxies with $L_{\text{bol}}/L_{\text{Edd}} \geq 0.01$ and repeated the study. More than 80 per cent of the galaxies were selected and the results were the same.

4 DISCUSSION

The test of the prevalence AGN with respect to the density is fully compatible with the hypothesised scenario in which the galaxy density does not play any role after the galaxy mass and the central sSFR are taken into account. The p -value is 2 per cent and the CMH ratio is very close to 1. If the sample is separated by sSFR the p -values are above 5 per cent. Given the size of the sample and the magnitude of the CMH ratio, we can consider that there is not any significant trend with respect to the density of galaxies. We showed in SBA13 how the trend is significant if only the mass is considered. Hence, the effect of the density and the central sSFR are strongly correlated. Additionally, we found the lack of a clear trend for the median of $\log(L_{[\text{O III}]} / M_{\text{BH}})$, which traces the activity level of the AGN, with respect to density. The main variation of the activity level is driven by the galaxy mass and the central sSFR. All of this is in agreement with the picture arising from the results of Li et al. (2008b) and Reichard et al. (2009) that the AGN activity depends on the cold gas supply to the nucleus and not on how it gets there. In higher galaxy density environments the gas supply to the galaxy as a whole is reduced, and reduced gas supply to the centre indirectly reduces AGN activity.

Our own study on the effect of one-on-one interactions is also broadly consistent with this picture. We find that the activity level of the AGN (as judged from the median of $\log(L_{[\text{O III}]} / M_{\text{BH}})$) is independent of the PCA2 parameter, once mass and sSFR are accounted for. This result is in agreement with that of Reichard et al. (2009), who

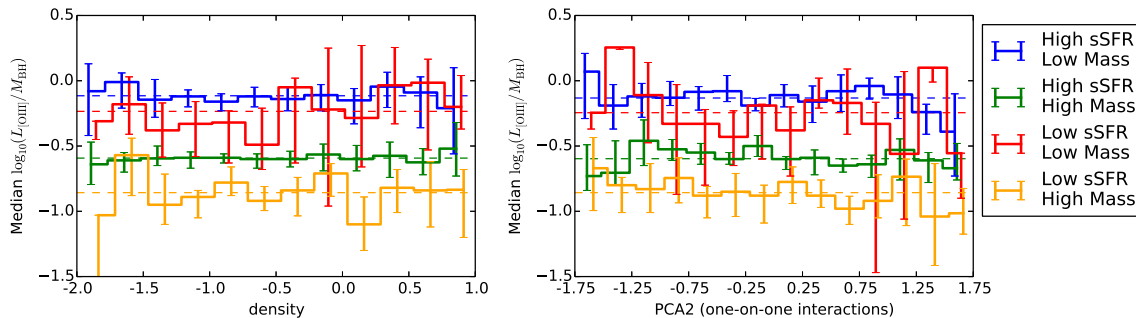


Figure 5. Activity level of the AGN traced by the median of the $\log(L_{\text{O III}}/M_{\text{BH}})$ with respect to the density and one-on-one interactions (PCA2) for each of the sub-samples. The error bars mark the 95 per cent confidence interval. The dashed lines mark the median for each sub-sample.

found that the activity level depends clearly on the stellar age (traced by D4000 and correlated with the sSFR; Brinchmann et al. 2004) but with little dependence on the lopsidedness of the galaxy (their Fig. 14). Our CMH test for the sample as a whole is also consistent with the lack of any trend between AGN prevalence and PCA2, in line with this picture. However, if the sample is separated into sub-samples some significant trends arise at a 20 to 30 per cent level. Although significant, they are small in comparison to some of the high ratio values found in SBA13 when central sSFR was not accounted for. The trends found do not directly fit into the previous model and suggest additional factors may be at play.

The increase found for low sSFR galaxies could be explained by the expected positive relation between the triggering of AGN and strong interactions present in theoretical models (e.g. Hopkins & Hernquist 2006). However, under this assumption a similar trend would also be expected for high sSFR galaxies and this is not the seen. A more likely explanation is the different time-scale between the triggering of the central star formation burst and the AGN (e.g. Li et al. 2008b; Darg et al. 2010; Wild et al. 2010). Wild et al. (2010) found that the growth of the black hole is delayed by about 250 Myr with respect to the start of the starburst. This time delay may be sufficient to weaken the correlation between central SF and AGN activity in interacting systems (high PCA2) and cause the observed trends: in interacting galaxies, AGN activity is less likely to occur when the sSFR is high (when the starburst is triggered) and more likely to be observed later, when the sSFR has dropped.

In general, we find that central sSFR and galaxy density are strongly correlated and one-on-one interactions play a secondary role on the triggering of AGN. This results are compatible with a scenario in which the presence of cold gas in the centre of a galaxy is the principal factor required for the triggering of radiatively efficient AGN. The cold gas supply to the central regions depends upon both the galaxy’s large-scale environment and any interactions. The AGN does not need one-on-one interactions to be triggered and can be fed via secular processes.

5 SUMMARY AND CONCLUSIONS

We presented a study of the relation between the prevalence of optical nuclear activity with respect to the environment in a sample of SDSS galaxies. We aimed to quantify the effect of different aspects of the environment on radiatively efficient nuclear activity. The study is based on a sample of ~ 270000 galaxies drawn from the DR7 of the SDSS. Two environmental parameters, the local density of galaxies and PCA2 which traces one-on-one interactions, were used. The mass and sSFR of the galaxy were considered as confounding factors of several stratified statistical tests. The sample was divided in sub-samples based on the mass and the sSFR when necessary and the significance of the prevalence of AGN with respect to the environmental parameters was obtained. We found that:

- (i) The dependence of the prevalence of AGN on the local galaxy density is practically null once both the mass and the sSFR are fixed. This indicates that AGN activity depends only on the availability of cold gas at the centre of a galaxy.
- (ii) The variation of the AGN activity level, traced by an Eddington-scaled accretion rate parameter, seems to be mainly driven by the galaxy mass and the central sSFR. Once their effect is taken into account, the effect of the density and one-on-one interactions is secondary at most.
- (iii) The effect of PCA2 (one-on-one interactions) is not significant if the sample is considered as a whole. However, a general homogeneous trend is not found and there are significant trends when the mass and sSFR sub-samples are considered separately: (a) a small positive trend on the prevalence of AGN with one-on-one interactions for galaxies with high mass and low sSFR, and, (b) a slight negative relation on the prevalence of AGN for low mass high sSFR galaxies with respect to one-on-one interactions. The interpretation of those trends may be related to the delay in the onset of an AGN after the galaxy interacts and the star formation is enhanced.

Overall, the effect of the local density of galaxies and of one-on-one interactions is minimal in both the prevalence of AGN activity and AGN luminosity, once the effects of mass and central star-formation are accounted for. This suggests that the level of nuclear activity depends primarily on the availability of cold gas in the nuclear regions of galaxies and that secular processes can drive the AGN activity in the majority of cases. Large scale environment and galaxy in-

teractions only affect AGN activity in an indirect manner, by influencing the central gas supply.

ACKNOWLEDGMENTS

JS and PNB are grateful for financial support from STFC. We thank the referee for quick and helpful comments.

This research made use of *ASTROPY*, a community-developed core Python package for Astronomy (Astropy Collaboration 2013); *IPYTHON* (Pérez & Granger 2007); *MATPLOTLIB* (Hunter 2007); *NUMPY* (Walt et al. 2011); *PANDAS* (McKinney 2010); *SCIPY* (Jones et al. 2001–) and *TOPCAT* (Taylor 2005).

Funding for the SDSS and SDSS-II has been provided by the Alfred P. Sloan Foundation, the Participating Institutions, the National Science Foundation, the U.S. Department of Energy, the National Aeronautics and Space Administration, the Japanese Monbukagakusho, the Max Planck Society, and the Higher Education Funding Council for England. The SDSS Web Site is <http://www.sdss.org/>. The SDSS is managed by the Astrophysical Research Consortium for the Participating Institutions. The Participating Institutions are the American Museum of Natural History, Astrophysical Institute Potsdam, University of Basel, University of Cambridge, Case Western Reserve University, University of Chicago, Drexel University, Fermilab, the Institute for Advanced Study, the Japan Participation Group, Johns Hopkins University, the Joint Institute for Nuclear Astrophysics, the Kavli Institute for Particle Astrophysics and Cosmology, the Korean Scientist Group, the Chinese Academy of Sciences (LAMOST), Los Alamos National Laboratory, the Max-Planck-Institute for Astronomy (MPIA), the Max-Planck-Institute for Astrophysics (MPA), New Mexico State University, Ohio State University, University of Pittsburgh, University of Portsmouth, Princeton University, the United States Naval Observatory, and the University of Washington.

REFERENCES

- Abazajian K. N. et al., 2009, *ApJS*, 182, 543
 Alonso M. S., Lambas D. G., Tissera P., Coldwell G., 2007, *MNRAS*, 375, 1017
 Astropy Collaboration et al., 2013, *A&A*, 558, A33
 Best P. N., Kauffmann G., Heckman T. M., Brinchmann J., Charlot S., Ivezić Ž., White S. D. M., 2005, *MNRAS*, 362, 25
 Brinchmann J., Charlot S., White S. D. M., Tremonti C., Kauffmann G., Heckman T., Brinkmann J., 2004, *MNRAS*, 351, 1151
 Carter B. J., Fabricant D. G., Geller M. J., Kurtz M. J., McLean B., 2001, *ApJ*, 559, 606
 Cattaneo A. et al., 2009, *Nature*, 460, 213
 Cochran W. G., 1954, *Biometrics*, 10, 417
 Darg D. W. et al., 2010, *MNRAS*, 401, 1552
 Ellison S. L., Patton D. R., Mendel J. T., Scudder J. M., 2011, *MNRAS*, 418, 2043
 Ferrarese L., Merritt D., 2000, *ApJ*, 539, L9
 Gebhardt K. et al., 2000, *ApJ*, 539, L13
 Heckman T. M., Best P. N., 2014, *ARA&A*, 58
 Hopkins P. F., Hernquist L., 2006, *ApJS*, 166, 1
 Hunter J. D., 2007, *Computing in Science & Engineering*, 9, 90
 Hwang H. S., Park C., Elbaz D., Choi Y. Y., 2012, *A&A*, 538, A15
 Jones E., Oliphant T., Peterson P. et al., 2001–, *SciPy: Open source scientific tools for Python*. [Online; accessed 2014-08-26]
 Kauffmann G. et al., 2003, *MNRAS*, 346, 1055
 Kauffmann G., White S. D. M., Heckman T. M., Ménard B., Brinchmann J., Charlot S., Tremonti C., Brinkmann J., 2004, *MNRAS*, 353, 713
 Kauffmann G. et al., 2007, *ApJS*, 173, 357
 Kewley L. J., Groves B., Kauffmann G., Heckman T., 2006, *MNRAS*, 372, 961
 Koulouridis E., Plionis M., Chavushyan V., Dultzin-Hacyan D., Krongold Y., Goudis C., 2006, *ApJ*, 639, 37
 LaMassa S. M., Heckman T. M., Ptak A., Urry C. M., 2013, *ApJ*, 765, L33
 Li C., Kauffmann G., Heckman T. M., Jing Y. P., White S. D. M., 2008a, *MNRAS*, 385, 1903
 Li C., Kauffmann G., Heckman T. M., White S. D. M., Jing Y. P., 2008b, *MNRAS*, 385, 1915
 Lintott C. J. et al., 2008, *MNRAS*, 389, 1179
 Liu X., Shen Y., Strauss M. A., 2012, *ApJ*, 745, 94
 Mantel N., Haenszel W., 1959, *Journal of the National Cancer Institute*, 22, 719
 Marconi A., Hunt L. K., 2003, *ApJ*, 589, L21
 McConnell N. J., Ma C. P., 2013, *ApJ*, 764, 184
 McKinney W., 2010, in S. van der Walt, J. Millman, eds, *Proceedings of the 9th Python in Science Conference*. pp. 51 – 56
 Miller C. J., Nichol R. C., Gómez P. L., Hopkins A. M., Bernardi M., 2003, *ApJ*, 597, 142
 Moles M., Marquez I., Perez E., 1995, *ApJ*, 438, 604
 Park C., Choi Y. Y., 2009, *ApJ*, 691, 1828
 Pérez F., Granger B. E., 2007, *Computing in Science and Engineering*, 9, 21
 Petrosian A. R., 1982, *Astrofizika*, 18, 548
 Reichard T. A., Heckman T. M., Rudnick G., Brinchmann J., Kauffmann G., Wild V., 2009, *ApJ*, 691, 1005
 Rogers B., Ferreras I., Kaviraj S., Pasquali A., Sarzi M., 2009, *MNRAS*, 399, 2172
 Sabater J., Verdes-Montenegro L., Leon S., Best P., Sulentic J., 2012, *A&A*, 545, A15
 Sabater J., Best P. N., Argudo-Fernández M., 2013, *MNRAS*, 430, 638
 Schawinski K., Dowlin N., Thomas D., Urry C. M., Edmondson E., 2010, *ApJ*, 714, L108
 Silverman J. D. et al., 2009, *ApJ*, 695, 171
 Strateva I. et al., 2001, *AJ*, 122, 1861
 Strauss M. A. et al., 2002, *AJ*, 124, 1810
 Tago E., Saar E., Tempel E., Einasto J., Einasto M., Nurmi P., Heinämäki P., 2010, *A&A*, 514, A102
 Tasse C., Röttgering H., Best P. N., 2011, *A&A*, 525, A127+
 Taylor M. B., 2005, in P. Shopbell, M. Britton, R. Ebert, eds, *Astronomical Data Analysis Software and Systems XIV. Astronomical Society of the Pacific Conference Series*, Vol. 347, p. 29
 Walt S. v. d., Colbert S. C., Varoquaux G., 2011, *Computing in Science & Engineering*, 13, 22

Wild V., Heckman T., Charlot S., 2010, MNRAS, 405, 933

Wolf B., 1955, Annals of Human Genetics, 19, 251